

# Spherical Mode-Based Analysis of Wireless Power Transfer Between Two Antennas

Yoon Goo Kim and Sangwook Nam, *Senior Member, IEEE*

**Abstract**—A method is presented to analyze the maximum power transfer efficiency of a wireless power transfer system and its electromagnetic fields via spherical modes. The Z-parameter and Y-parameter for two coupled antennas are derived using the antenna scattering matrix and an addition theorem. In addition, formulas for calculating the maximum power transfer efficiency and optimum load impedance are presented. A formula is derived to calculate the electromagnetic field generated by a wireless power transfer system from the antenna scattering matrix.

**Index Terms**—Addition theorem, antenna mutual coupling, spherical mode, wireless power transfer.

## I. INTRODUCTION

OVER the last century, many researchers have attempted to transmit electrical energy without the use of wires [1]–[6]. In the past, wireless power transfer using far field, which is used in long-range power transfer, has been studied [1]. Currently, wireless power transfer using near field is receiving a considerable amount of attention for short-range power transfer [2]–[6]. Several analytical models for wireless power transfer using near field have been proposed. These models include an analysis using coupled-mode theory [2], an analysis using an equivalent circuit [3], [4], and an analysis using filter theory [5]. These models typically require a solution of a boundary value problem in the presence of the detailed geometry of all antennas. It may be desirable to describe wireless power transfer in terms of a closed-form equation using the parameters of an isolated antenna. When this is done, it can help us to understand the factors that affect wireless power transfer and to design an efficient wireless power transfer system. Analysis using spherical modes is suitable for this purpose. Previous research [6] has used spherical modes to analyze the wireless power transfer between two identical canonical-minimum-scattering antennas that generate only fundamental modes. This paper examines the general case in which two different antennas generate arbitrary spherical modes and have arbitrary scattering properties.

To investigate the characteristics of wireless power transfer, we should analyze the coupling between antennas, because power is transferred from antenna to antenna through the coupling phenomenon. Coupling between antennas is described

Manuscript received February 27, 2013; revised September 18, 2013; accepted November 17, 2013. Date of publication March 19, 2014; date of current version May 29, 2014. This research was funded by the MSIP (Ministry of Science, ICT & Future Planning), Korea in the ICT R&D Program 2013.

The authors are with the Department of Electrical and Computer Engineering, Seoul National University, Seoul, 151-742 Korea (e-mail: scika@ael.snu.ac.kr; snam@snu.ac.kr).

Color versions of one or more of the figures in this paper are available online at <http://ieeexplore.ieee.org>.

Digital Object Identifier 10.1109/TAP.2014.2312419

by the S-parameter, Z-parameter, or Y-parameter. Previous studies [7]–[9] have derived the S-parameter, Z-parameter, and Y-parameter between antennas using the antenna scattering matrix for the analysis of near-field measurement and antenna arrays. We apply the antenna-scattering-matrix theory to wireless power transfer. In this paper, we derive the Z-parameter and Y-parameter between two antennas in free-space using the antenna scattering matrix and an addition theorem.

One of the most important parameters in wireless power transfer is power transfer efficiency. Power transfer efficiency depends on load impedance. We determine both a load impedance for which power transfer efficiency is maximized and a formula for calculating maximum power transfer efficiency from the Z-parameter.

To use wireless power transfer in practice, the effects of wireless power transfer on human bodies and electronic devices should be investigated. In addition, such systems must adhere to relevant regulations, such as EMC regulations. Therefore, it is necessary to determine the electromagnetic fields near wireless power transfer systems. In this paper, we derive a formula for calculating the electromagnetic field generated by two coupled antennas in free-space. Finally, the proposed formula is validated using a simulation.

Throughout this paper, it is assumed that an antenna has one feeding port. The  $e^{j\omega t}$  time dependence is used throughout this paper.

## II. ANTENNA SCATTERING MATRIX

The electric field and magnetic field outside a sphere enclosing an antenna can be expressed as a superposition of spherical modes (Appendix A). The coefficients of the incident and reflected waves at the feeding port of an antenna and the coefficients of the incoming and outgoing spherical modes are related by the following antenna-scattering-matrix equation:

$$\begin{bmatrix} w \\ \mathbf{b} \end{bmatrix} = \begin{bmatrix} \Gamma & \mathbf{R} \\ \mathbf{T} & \mathbf{S} \end{bmatrix} \begin{bmatrix} v \\ \mathbf{a} \end{bmatrix}. \quad (1)$$

Here,  $v$  is the coefficient of an incident power wave at the feeding port, and  $w$  is the coefficient of a reflected power wave at the feeding port. The definition of power waves is presented in [10]. The antenna scattering matrix used in this paper is slightly different from the conventional antenna scattering matrix [7]; in the conventional antenna scattering matrix,  $v$  and  $w$  are the coefficients of traveling waves.  $\mathbf{a}$  denotes a column matrix containing the coefficients of the incoming spherical modes, and  $\mathbf{b}$  denotes a column matrix containing the coefficients of the outgoing spherical modes for the total field (incident field + scattered field).  $\Gamma$  is the reflection coefficient, and  $\mathbf{T}$ ,  $\mathbf{R}$ , and  $\mathbf{S}$  describe the transmitting, receiving, and

scattering properties of the antenna, respectively.  $\mathbf{T}$  and  $\mathbf{R}$  are called the modal transmitting pattern and modal receiving pattern, respectively [9]. The mode functions are normalized such that one half of the square of the absolute value of the coefficient is equal to the power carried by the wave.

$(s, m, n)$  denote the indices of spherical modes, where  $s = 1$  denotes the TE mode, and  $s = 2$  denotes the TM mode, while  $m$  and  $n$  are the indices defined in Appendix A. The ordering of the mode coefficients is arbitrary. In this paper, the modes are ordered as follows:

$$\begin{aligned} & \text{TE}_{-11}, \text{TE}_{01}, \text{TE}_{11}, \text{TM}_{-11}, \text{TM}_{01}, \text{TM}_{11}, \text{TE}_{-22}, \text{TE}_{-12}, \\ & \text{TE}_{02}, \text{TE}_{12}, \text{TE}_{22}, \text{TM}_{-22}, \text{TM}_{-12}, \text{TM}_{02}, \text{TM}_{12}, \\ & \text{TM}_{22}, \dots, \text{TE}_{mn}, \dots, \text{TM}_{mn}, \dots \end{aligned}$$

The  $q$ th mode is the mode with index  $(s, m, n)$  that satisfies the following equation:

$$q = (s - 1)(2n + 1) + (2n - 1)(n + 1) + m. \quad (2)$$

The modal receiving pattern of a reciprocal antenna can be found from the modal transmitting pattern.  $\mathbf{R}$  is determined from the following equation [7, p. 36]:

$$R_{s,m,n} = (-1)^m T_{s,-m,n} \quad (3)$$

where  $T_{s,m,n}$  and  $R_{s,m,n}$  are the elements of  $\mathbf{T}$  and  $\mathbf{R}$ , respectively, and the subscript denotes the mode indices. In [7], (3) was derived for the case in which  $v$  and  $w$  are the coefficients of traveling waves, and a feed waveguide is completely enclosed by a conductor except for a reference plane. Equation (3) is also valid when  $v$  and  $w$  are the coefficients of power waves<sup>1</sup> or when an antenna is excited at a gap.

An antenna that does not scatter electromagnetic fields when its feeding port is open-circuited is called a canonical-minimum-scattering antenna [11]. The expression for  $\mathbf{S}$  for a canonical-minimum-scattering antenna is [12, eq. 16]

$$\mathbf{S} = \mathbf{I} - \frac{1}{1 - \Gamma} \mathbf{TR} \quad (4)$$

where  $\mathbf{I}$  is the identity matrix.

### III. MUTUAL COUPLING BETWEEN TWO ANTENNAS

#### A. Network Representation of Coupled Antennas

We place antenna 1 at the origin of coordinate system 1 ( $x_1, y_1, z_1$  axes) and antenna 2 at the origin of coordinate system 3 ( $x_3, y_3, z_3$  axes), as shown in Fig. 1. Coordinate system 2 ( $x_2, y_2, z_2$  axes) is obtained by translating coordinate system 1, and coordinate system 3 is obtained by rotating coordinate system 2. The origin of coordinate system 2 is located at  $(r, \theta, \phi)$  in the spherical coordinates of coordinate system 1, and the rotation of the coordinates is described by the Euler angles  $(\chi_0, \theta_0, \phi_0)$  [7, App. A2]. It is assumed that the two minimum spheres, one enclosing each antenna, do not overlap.

<sup>1</sup>When the power wave is used,  $(v + w)$  in [7, eq. (2.81)] is replaced by  $(Z_R^* + Z_R w) / \sqrt{Z_0 \text{Re}(Z_R)}$  and  $(v - w)$  in [7, eq. (2.82)] is replaced by  $\sqrt{Z_0} + (v - w) / \sqrt{\text{Re}(Z_R)}$ , where  $Z_0$  is the real characteristic impedance of a feed waveguide and  $Z_R$  is the reference impedance. Then, the same result as that for the traveling wave is derived.

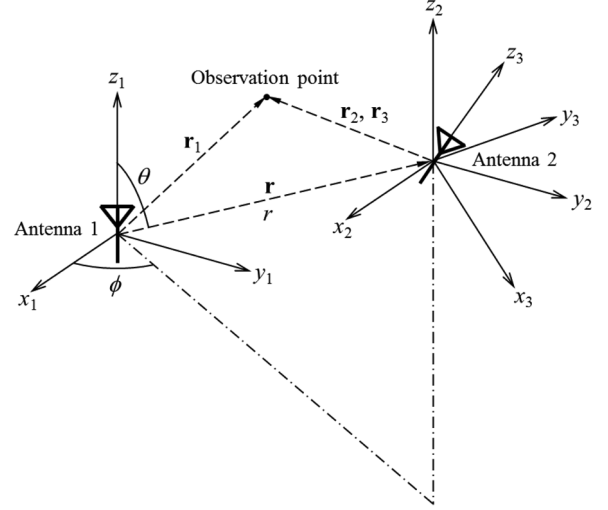


Fig. 1. Coordinate systems and antennas.

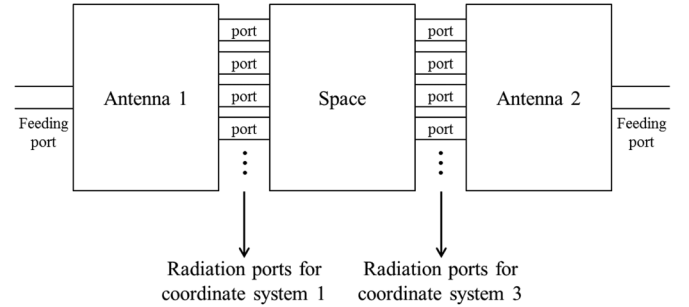


Fig. 2. Network representation of two coupled antennas.

The coupling between the two antennas is expressed by the Z-parameter, as follows:

$$v_1 = Z_{11}i_1 + Z_{12}i_2 \quad (5a)$$

$$v_2 = Z_{21}i_1 + Z_{22}i_2 \quad (5b)$$

or the Y-parameter, as follows:

$$i_1 = Y_{11}v_1 + Y_{12}v_2 \quad (6a)$$

$$i_2 = Y_{21}v_1 + Y_{22}v_2 \quad (6b)$$

where  $v_1$  and  $v_2$  are the voltages at the feeding ports of antenna 1 and antenna 2, respectively, and  $i_1$  and  $i_2$  are the currents at the feeding ports of antenna 1 and antenna 2, respectively. The coupling of the two antennas can be considered as a cascade of three networks, as shown in Fig. 2. Two of the networks are the antennas' networks, and the intermediate network represents the space outside the two spheres that surround antenna 1 and antenna 2.

#### B. Spherical Mode Coefficient Conversion

In this section, we determine the relation between the spherical mode coefficients with respect to coordinate system 1 and the spherical mode coefficients with respect to coordinate system 3. Let the coefficient of the  $q$ th incoming spherical mode in coordinate system  $p$  be  $a_q^{(p)}$  and the coefficient of the  $q$ th outgoing spherical mode in coordinate system  $p$  be  $b_q^{(p)}$ . Let  $\mathbf{a}^{(p)}$  and  $\mathbf{b}^{(p)}$  be column matrices and the  $q$ th elements of  $\mathbf{a}^{(p)}$  and  $\mathbf{b}^{(p)}$  be  $a_q^{(p)}$  and  $b_q^{(p)}$ , respectively. The total field consists

of the field generated by the current on antenna 1 and the field generated by the current on antenna 2 when there is no incident field outside the two antennas. In the sphere that is centered at the origin of coordinate system 1 and has radius  $r$ , the field generated by antenna 2 is composed of incoming and outgoing spherical modes with respect to coordinate system 1, and the coefficients of the incoming and outgoing spherical modes are equal. The coefficient  $a_q^{(1)}$  of the  $q$ th incoming spherical mode in coordinate system 1 is purely due to the current on antenna 2. Therefore, the coefficient of the  $q$ th outgoing spherical mode generated by the current on antenna 1 alone is  $b_q^{(1)} - a_q^{(1)}$  in coordinate system 1.  $a_p^{(2)}$  can be expanded in terms of  $b_q^{(1)} - a_q^{(1)}$  using the translational addition theorem:

$$a_p^{(2)} = \sum_{q=1}^{\infty} \frac{1}{2} G_{pq}^T(r, \theta, \phi) \left( b_q^{(1)} - a_q^{(1)} \right) \quad (7)$$

where  $G_{pq}^T$  is defined by

$$G_{pq}^T(r, \theta, \phi) = \begin{cases} A_{\mu\nu, mn}^{(4)}(r, \theta, \phi) & \text{when } s = \sigma \\ B_{\mu\nu, mn}^{(4)}(r, \theta, \phi) & \text{when } s \neq \sigma \end{cases} \quad (8)$$

where  $A_{\mu\nu, mn}^{(4)}(r, \theta, \phi)$  and  $B_{\mu\nu, mn}^{(4)}(r, \theta, \phi)$  are functions defined in Appendix B.  $(\sigma, \mu, \nu)$  is the mode index,  $p = (\sigma - 1)(2\nu + 1) + (2\nu - 1)(\nu + 1) + \mu$ , and  $q$  satisfies (2). Equation (7) can be written in matrix form

$$\mathbf{a}^{(2)} = \frac{1}{2} \mathbf{G}^T(r, \theta, \phi) \left( \mathbf{b}^{(1)} - \mathbf{a}^{(1)} \right) \quad (9)$$

where the element in the  $p$ th row and  $q$ th column of  $\mathbf{G}^T$  is  $G_{pq}^T$ . The coefficient  $a_p^{(3)}$  of the  $p$ th incoming spherical mode in coordinate system 3 can be expanded in terms of  $a_q^{(2)}$  using the rotational addition theorem

$$a_p^{(3)} = \sum_{q=1}^{\infty} G_{pq}^R(\chi_0, \theta_0, \phi_0) a_q^{(2)} \quad (10)$$

where  $G_{pq}^R$  is defined as

$$G_{pq}^R(\chi_0, \theta_0, \phi_0) = \begin{cases} D_{\mu\nu, mn}^n(\chi_0, \theta_0, \phi_0) & \text{when } s = \sigma \text{ and } n = \nu \\ 0 & \text{otherwise} \end{cases} \quad (11)$$

where  $D_{\mu\nu, mn}^n(\chi_0, \theta_0, \phi_0)$  is a function defined in Appendix C, and  $p$  and  $q$  are given by the same equations as those used in (8). Equation (10) can be written in matrix form

$$\mathbf{a}^{(3)} = \mathbf{G}^R(\chi_0, \theta_0, \phi_0) \mathbf{a}^{(2)} \quad (12)$$

where the element in the  $p$ th row and  $q$ th column of  $\mathbf{G}^R$  is  $G_{pq}^R$ . Therefore, the relation between  $\mathbf{b}^{(1)} - \mathbf{a}^{(1)}$  and  $\mathbf{a}^{(3)}$  can be written as

$$\begin{aligned} \mathbf{a}^{(3)} &= \frac{1}{2} \mathbf{G}^R(\chi_0, \theta_0, \phi_0) \mathbf{G}^T(r, \theta, \phi) \left( \mathbf{b}^{(1)} - \mathbf{a}^{(1)} \right) \\ &= \frac{1}{2} \mathbf{G}^+ \left( \mathbf{b}^{(1)} - \mathbf{a}^{(1)} \right). \end{aligned} \quad (13)$$

Likewise, the relation between  $\mathbf{b}^{(3)} - \mathbf{a}^{(3)}$  and  $\mathbf{a}^{(1)}$  can be written as

$$\begin{aligned} \mathbf{a}^{(1)} &= \frac{1}{2} \mathbf{G}^T(r, \pi - \theta, \pi + \phi) \mathbf{G}^R(-\phi_0, -\theta_0, -\chi_0) \left( \mathbf{b}^{(3)} - \mathbf{a}^{(3)} \right) \\ &= \frac{1}{2} \mathbf{G}^- \left( \mathbf{b}^{(3)} - \mathbf{a}^{(3)} \right). \end{aligned} \quad (14)$$

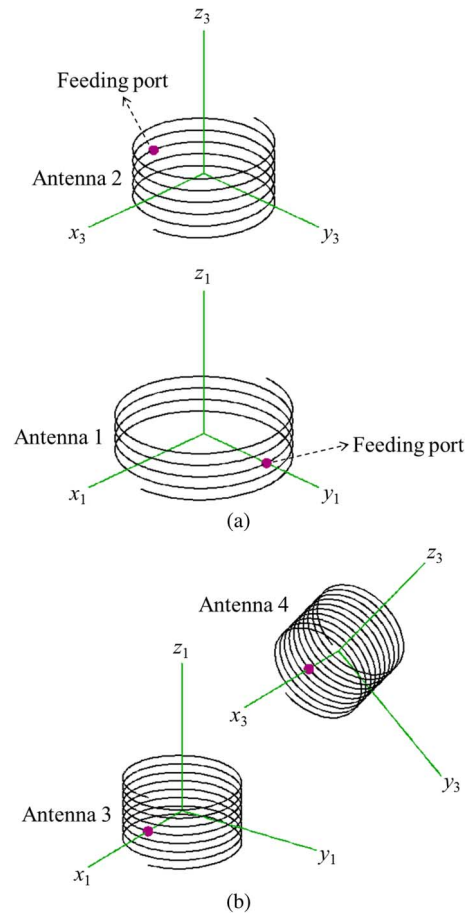


Fig. 3. Antenna configurations and coordinate systems: (a) antenna 1 and antenna 2 and (b) antenna 3 and antenna 4.

### C. Z-Parameter and Y-Parameter Between Two Antennas

Let the antenna scattering matrices of antenna 1 and antenna 2 be

$$\mathbf{S}^{(1)} = \begin{bmatrix} \Gamma_1 & \mathbf{R}_1 \\ \mathbf{T}_1 & \mathbf{S}_1 \end{bmatrix}, \quad \mathbf{S}^{(2)} = \begin{bmatrix} \Gamma_2 & \mathbf{R}_2 \\ \mathbf{T}_2 & \mathbf{S}_2 \end{bmatrix} \quad (15)$$

respectively, where  $\mathbf{S}^{(1)}$  and  $\mathbf{S}^{(2)}$  are referred to as coordinate system 1 and coordinate system 3, respectively. It is assumed that the number of spherical modes in the antenna scattering matrices of antenna 1 and antenna 2 are the same. Let the reference impedances of the feeding ports of antenna 1 and antenna 2 be  $Z_{R1}$  and  $Z_{R2}$ , respectively. The antenna-scattering-matrix equations of antenna 1 and antenna 2 can be expressed as follows:

$$\begin{bmatrix} \frac{(v_1 - Z_{R1}^* i_1)}{2\sqrt{\text{Re}(Z_{R1})}} \\ \mathbf{b}^{(1)} \end{bmatrix} = \begin{bmatrix} \Gamma_1 & \mathbf{R}_1 \\ \mathbf{T}_1 & \mathbf{S}_1 \end{bmatrix} \begin{bmatrix} \frac{(v_1 - Z_{R1} i_1)}{2\sqrt{\text{Re}(Z_{R1})}} \\ \mathbf{a}^{(1)} \end{bmatrix} \quad (16a)$$

$$\begin{bmatrix} \frac{(v_2 - Z_{R2}^* i_2)}{2\sqrt{\text{Re}(Z_{R2})}} \\ \mathbf{b}^{(3)} \end{bmatrix} = \begin{bmatrix} \Gamma_2 & \mathbf{R}_2 \\ \mathbf{T}_2 & \mathbf{S}_2 \end{bmatrix} \begin{bmatrix} \frac{(v_2 - Z_{R2} i_2)}{2\sqrt{\text{Re}(Z_{R2})}} \\ \mathbf{a}^{(3)} \end{bmatrix} \quad (16b)$$

The Z-parameter of the two coupled antennas can be obtained by solving (13), (14), and (16) and is given by the following:

$$Z_{11} = \frac{Z_{R1}^* + Z_{R1}\Gamma_1}{1 - \Gamma_1} + \frac{\text{Re}(Z_{R1})}{2(1 - \Gamma_1)^2} \mathbf{R}_1 \mathbf{G}^- \times \left[ \mathbf{I} - \frac{1}{4} \mathbf{P}_2^O \mathbf{G}^+ \mathbf{P}_1^O \mathbf{G}^- \right]^{-1} \mathbf{P}_2^O \mathbf{G}^+ \mathbf{T}_1 \quad (17a)$$

$$Z_{12} = \frac{\sqrt{\text{Re}(Z_{R1})\text{Re}(Z_{R2})}}{(1 - \Gamma_1)(1 - \Gamma_2)} \mathbf{R}_1 \mathbf{G}^- \times \left[ \mathbf{I} - \frac{1}{4} \mathbf{P}_2^O \mathbf{G}^+ \mathbf{P}_1^O \mathbf{G}^- \right]^{-1} \mathbf{T}_2 \quad (17b)$$

$$Z_{21} = \frac{\sqrt{\text{Re}(Z_{R1})\text{Re}(Z_{R2})}}{(1 - \Gamma_1)(1 - \Gamma_2)} \mathbf{R}_2 \mathbf{G}^+ \times \left[ \mathbf{I} - \frac{1}{4} \mathbf{P}_1^O \mathbf{G}^- \mathbf{P}_2^O \mathbf{G}^+ \right]^{-1} \mathbf{T}_1 \quad (17c)$$

$$Z_{22} = \frac{Z_{R2}^* + Z_{R2}\Gamma_2}{1 - \Gamma_2} + \frac{\text{Re}(Z_{R2})}{2(1 - \Gamma_2)^2} \mathbf{R}_2 \mathbf{G}^+ \times \left[ \mathbf{I} - \frac{1}{4} \mathbf{P}_1^O \mathbf{G}^- \mathbf{P}_2^O \mathbf{G}^+ \right]^{-1} \mathbf{P}_1^O \mathbf{G}^- \mathbf{T}_2 \quad (17d)$$

where

$$\mathbf{P}_1^O = \mathbf{S}_1 + \frac{1}{1 - \Gamma_1} \mathbf{T}_1 \mathbf{R}_1 - \mathbf{I} \quad (18a)$$

$$\mathbf{P}_2^O = \mathbf{S}_2 + \frac{1}{1 - \Gamma_2} \mathbf{T}_2 \mathbf{R}_2 - \mathbf{I} \quad (18b)$$

When the antennas are canonical-minimum-scattering antennas, from (4), the Z-parameter reduces to the following:

$$Z_{11} = \frac{Z_{R1}^* + Z_{R1}\Gamma_1}{1 - \Gamma_1} = Z_{in1} \quad (19a)$$

$$Z_{12} = \frac{\sqrt{\text{Re}(Z_{R1})\text{Re}(Z_{R2})}}{(1 - \Gamma_1)(1 - \Gamma_2)} \mathbf{R}_1 \mathbf{G}^- \mathbf{T}_2 \quad (19b)$$

$$Z_{21} = \frac{\sqrt{\text{Re}(Z_{R1})\text{Re}(Z_{R2})}}{(1 - \Gamma_1)(1 - \Gamma_2)} \mathbf{R}_2 \mathbf{G}^+ \mathbf{T}_1 \quad (19c)$$

$$Z_{22} = \frac{Z_{R2}^* + Z_{R2}\Gamma_2}{1 - \Gamma_2} = Z_{in2} \quad (19d)$$

where  $Z_{in1}$  and  $Z_{in2}$  are the input impedances of antenna 1 and antenna 2, respectively.

The Y-parameter is given by the following:

$$Y_{11} = \frac{1 - \Gamma_1}{Z_{R1}^* + Z_{R1}\Gamma_1} - \frac{\text{Re}(Z_{R1})}{2(Z_{R1}^* + Z_{R1}\Gamma_1)^2} \mathbf{R}_1 \mathbf{G}^- \times \left[ \mathbf{I} - \frac{1}{4} \mathbf{P}_2^S \mathbf{G}^+ \mathbf{P}_1^S \mathbf{G}^- \right]^{-1} \mathbf{P}_2^S \mathbf{G}^+ \mathbf{T}_1 \quad (20a)$$

$$Y_{12} = \frac{-\sqrt{\text{Re}(Z_{R1})\text{Re}(Z_{R2})}}{(Z_{R1}^* + Z_{R1}\Gamma_1)(Z_{R2}^* + Z_{R2}\Gamma_2)} \mathbf{R}_1 \mathbf{G}^- \times \left[ \mathbf{I} - \frac{1}{4} \mathbf{P}_2^S \mathbf{G}^+ \mathbf{P}_1^S \mathbf{G}^- \right]^{-1} \mathbf{T}_2 \quad (20b)$$

$$Y_{21} = \frac{-\sqrt{\text{Re}(Z_{R1})\text{Re}(Z_{R2})}}{(Z_{R1}^* + Z_{R1}\Gamma_1)(Z_{R2}^* + Z_{R2}\Gamma_2)} \mathbf{R}_2 \mathbf{G}^+ \times \left[ \mathbf{I} - \frac{1}{4} \mathbf{P}_1^S \mathbf{G}^- \mathbf{P}_2^S \mathbf{G}^+ \right]^{-1} \mathbf{T}_1 \quad (20c)$$

$$Y_{22} = \frac{1 - \Gamma_2}{Z_{R2}^* + Z_{R2}\Gamma_2} - \frac{\text{Re}(Z_{R2})}{2(Z_{R2}^* + Z_{R2}\Gamma_2)^2} \mathbf{R}_2 \mathbf{G}^+ \times \left[ \mathbf{I} - \frac{1}{4} \mathbf{P}_1^S \mathbf{G}^- \mathbf{P}_2^S \mathbf{G}^+ \right]^{-1} \mathbf{P}_1^S \mathbf{G}^- \mathbf{T}_2 \quad (20d)$$

where

$$\mathbf{P}_1^S = \mathbf{S}_1 - \frac{Z_{R1}}{Z_{R1}^* + Z_{R1}\Gamma_1} \mathbf{T}_1 \mathbf{R}_1 - \mathbf{I} \quad (21a)$$

$$\mathbf{P}_2^S = \mathbf{S}_2 - \frac{Z_{R2}}{Z_{R2}^* + Z_{R2}\Gamma_2} \mathbf{T}_2 \mathbf{R}_2 - \mathbf{I} \quad (21b)$$

#### IV. MAXIMUM POWER TRANSFER EFFICIENCY AND OPTIMUM LOAD IMPEDANCE

If the Z-parameter is given, the load impedance at which the maximum power is transferred and the maximum power transfer efficiency can be calculated. Let a load impedance  $Z_L$  be connected to the feeding port of antenna 2, and let a source be connected to the feeding port of antenna 1. The power transfer efficiency (PTE) is defined as

$$\text{PTE} = \frac{P_L}{P_{in}} = \frac{\text{Re}(Z_L)}{\text{Re}(Z_{in})} \left| \frac{Z_{21}}{Z_{22} + Z_L} \right|^2 \quad (22)$$

where  $P_L$  is the power dissipated in the load,  $P_{in}$  is the power that enters the network, and  $Z_{in}$  is the input impedance observed at the feeding port of antenna 1. The power transfer efficiency is maximized when  $Z_L$  satisfies the following equations:

$$\frac{\partial \text{PTE}}{\partial \text{Re}(Z_L)} = 0, \quad \frac{\partial \text{PTE}}{\partial \text{Im}(Z_L)} = 0. \quad (23)$$

The  $\text{Re}(Z_L)$  and  $\text{Im}(Z_L)$  that satisfy the above equations are as follows:

$$\text{Re}(Z_L) = \sqrt{\text{Re}(Z_{22})^2 - \frac{\text{Re}(Z_{22})}{\text{Re}(Z_{11})} \text{Re}(Z_{12}Z_{21}) - \frac{\text{Im}(Z_{12}Z_{21})^2}{4\text{Re}(Z_{11})^2}} \quad (24a)$$

$$\text{Im}(Z_L) = \frac{\text{Im}(Z_{12}Z_{21})}{2\text{Re}(Z_{11})} - \text{Im}(Z_{22}) \quad (24b)$$

when  $\text{Re}(Z_{11}) \neq 0$ . The maximum power transfer efficiency ( $\text{PTE}^{\max}$ ) is given by the following equation:

$$\text{PTE}^{\max} = \frac{|X_2|^2}{2 - \text{Re}(X_1 X_2) + \sqrt{4 - 4\text{Re}(X_1 X_2) - \text{Im}(X_1 X_2)^2}} \quad (25)$$

where

$$X_1 = \frac{Z_{12}}{\sqrt{\text{Re}(Z_{11})\text{Re}(Z_{22})}}, \quad X_2 = \frac{Z_{21}}{\sqrt{\text{Re}(Z_{11})\text{Re}(Z_{22})}} \quad (26)$$

## V. ELECTROMAGNETIC FIELD GENERATED BY A WIRELESS POWER TRANSFER SYSTEM

As explained in Section III-B, the spherical mode coefficients produced by the current on antenna 1 alone are  $\mathbf{b}^{(1)} - \mathbf{a}^{(1)}$  in coordinate system 1, and the spherical mode coefficients produced by the current on antenna 2 alone are  $\mathbf{b}^{(3)} - \mathbf{a}^{(3)}$  in coordinate system 3. Solving (13), (14), and (16), we obtain  $\mathbf{b}^{(1)} - \mathbf{a}^{(1)}$  and  $\mathbf{b}^{(3)} - \mathbf{a}^{(3)}$ .

$$\begin{aligned} & \mathbf{b}^{(1)} - \mathbf{a}^{(1)} \\ &= \left[ \mathbf{I} - \frac{1}{4} \mathbf{P}_1^0 \mathbf{G}^- \mathbf{P}_2^0 \mathbf{G}^+ \right]^{-1} \\ & \quad \times \left[ \frac{\sqrt{\text{Re}(Z_{R1})}}{1 - \Gamma_1} \mathbf{T}_1 i_1 + \frac{\sqrt{\text{Re}(Z_{R2})}}{2(1 - \Gamma_2)} \mathbf{P}_1^0 \mathbf{G}^- \mathbf{T}_2 i_2 \right] \end{aligned} \quad (27a)$$

$$\begin{aligned} & \mathbf{b}^{(3)} - \mathbf{a}^{(3)} \\ &= \left[ \mathbf{I} - \frac{1}{4} \mathbf{P}_2^0 \mathbf{G}^+ \mathbf{P}_1^0 \mathbf{G}^- \right]^{-1} \\ & \quad \times \left[ \frac{\sqrt{\text{Re}(Z_{R2})}}{1 - \Gamma_2} \mathbf{T}_2 i_2 + \frac{\sqrt{\text{Re}(Z_{R1})}}{2(1 - \Gamma_1)} \mathbf{P}_2^0 \mathbf{G}^+ \mathbf{T}_1 i_1 \right] \end{aligned} \quad (27b)$$

An alternate formula is

$$\begin{aligned} & \mathbf{b}^{(1)} - \mathbf{a}^{(1)} \\ &= \left[ \mathbf{I} - \frac{1}{4} \mathbf{P}_1^S \mathbf{G}^- \mathbf{P}_2^S \mathbf{G}^+ \right]^{-1} \\ & \quad \cdot \left[ \frac{\sqrt{\text{Re}(Z_{R1})}}{Z_{R1}^* + Z_{R1} \Gamma_1} \mathbf{T}_1 v_1 + \frac{\sqrt{\text{Re}(Z_{R2})}}{2(Z_{R2}^* + Z_{R2} \Gamma_2)} \mathbf{P}_1^S \mathbf{G}^- \mathbf{T}_2 v_2 \right] \end{aligned} \quad (28a)$$

$$\begin{aligned} & \mathbf{b}^{(3)} - \mathbf{a}^{(3)} \\ &= \left[ \mathbf{I} - \frac{1}{4} \mathbf{P}_2^S \mathbf{G}^+ \mathbf{P}_1^S \mathbf{G}^- \right]^{-1} \\ & \quad \cdot \left[ \frac{\sqrt{\text{Re}(Z_{R2})}}{Z_{R2}^* + Z_{R2} \Gamma_2} \mathbf{T}_2 v_2 + \frac{\sqrt{\text{Re}(Z_{R1})}}{2(Z_{R1}^* + Z_{R1} \Gamma_1)} \mathbf{P}_2^S \mathbf{G}^+ \mathbf{T}_1 v_1 \right] \end{aligned} \quad (28b)$$

If the antennas are canonical-minimum-scattering antennas, (27) becomes

$$\mathbf{b}^{(1)} - \mathbf{a}^{(1)} = \frac{\sqrt{\text{Re}(Z_{R1})}}{1 - \Gamma_1} \mathbf{T}_1 i_1 \quad (29a)$$

$$\mathbf{b}^{(3)} - \mathbf{a}^{(3)} = \frac{\sqrt{\text{Re}(Z_{R2})}}{1 - \Gamma_2} \mathbf{T}_2 i_2. \quad (29b)$$

From (27) or (28) and the spherical mode functions in Appendix A, we can calculate electromagnetic field generated by a wireless power transfer system.

When antenna 2 is open-circuited and antenna 1 is excited with a current of 1 A, the spherical mode coefficients produced by the current on antenna 1 alone are denoted by  $\mathbf{b}_1^{o2}$ , and the spherical mode coefficients produced by the current on antenna 2 alone are denoted by  $\mathbf{b}_2^{o2}$ . When antenna 1 is open-circuited and antenna 2 is excited with a current of 1 A, the spherical mode coefficients produced by the current on antenna 2 alone are denoted by  $\mathbf{b}_2^{o1}$ , and the spherical mode coefficients produced by

TABLE I  
COEFFICIENTS OF DOMINANT SPHERICAL MODES AND INPUT IMPEDANCE

	Antenna 1	Antenna 2
TE <sub>01</sub> Mode	-0.448	-0.359
TM <sub>01</sub> Mode	-0.248	-0.318
Input impedance (Ω)	0.546 + j102	0.427 - j42.25

TABLE II  
COEFFICIENTS OF DOMINANT SPHERICAL MODES AND INPUT IMPEDANCE

	Antenna 3	Antenna 4
TE <sub>01</sub> Mode	-0.0439	-0.0400
TM <sub>01</sub> Mode	-0.0969	-0.111
Input impedance (Ω)	0.341 - j1187	0.351 - j1252

the current on antenna 1 alone are denoted by  $\mathbf{b}_1^{o1}$ . Then, (17) can be written as follows:

$$Z_{11} = \frac{Z_{R1}^* + Z_{R1} \Gamma_1}{1 - \Gamma_1} + \frac{\sqrt{\text{Re}(Z_{R1})}}{1 - \Gamma_1} \mathbf{R}_1 \mathbf{G}^- \mathbf{b}_2^{o2} \quad (30a)$$

$$Z_{12} = \frac{\sqrt{\text{Re}(Z_{R1})}}{1 - \Gamma_1} \mathbf{R}_1 \mathbf{G}^- \mathbf{b}_2^{o1} \quad (30b)$$

$$Z_{21} = \frac{\sqrt{\text{Re}(Z_{R2})}}{1 - \Gamma_2} \mathbf{R}_2 \mathbf{G}^+ \mathbf{b}_1^{o2} \quad (30c)$$

$$Z_{22} = \frac{Z_{R2}^* + Z_{R2} \Gamma_2}{1 - \Gamma_2} + \frac{\sqrt{\text{Re}(Z_{R2})}}{1 - \Gamma_2} \mathbf{R}_2 \mathbf{G}^+ \mathbf{b}_1^{o1}. \quad (30d)$$

## VI. NUMERICAL RESULTS AND VALIDATION

To verify the formula, we calculated the Z-parameter, Y-parameter, and maximum power transfer efficiency of a wireless power transfer system and the electromagnetic field near a wireless power transfer system using the formulas presented in this paper and compared the results with those obtained using the EM simulator FEKO. We designed four helical antennas. For antenna 1, the radius was 30 cm, the height was 20 cm, and the number of turns was 4.5. For antenna 2, the radius was 24 cm, the height was 25 cm, and the number of turns was 5.5. For antenna 3, the radius was 8 cm, the height was 10 cm, and the number of turns was 8. For antenna 4, the radius was 7 cm, the height was 12 cm, and the number of turns was 10. The wire used in all the antennas was made of copper. The diameter of the cross section of the wire used in antennas 1 and 2 was 4 mm, and the diameter of the cross section of the wire used in antennas 3 and 4 was 1 mm. All the antennas were fed at the center of the wire. The centers of antennas 1 and 3 were located at the origin of coordinate system 1, and the axes of antennas 1 and 3 coincided with the  $z_1$ -axis. The centers of antennas 2 and 4 were located at the origin of coordinate system 3, and the axes of antennas 2 and 4 coincided with the  $z_3$ -axis. The origin of coordinate system 3 was located at  $(r, \theta, \phi)$  with respect to coordinate system 1.

We extracted the current distributions of the helical antennas using FEKO. We calculated  $\mathbf{T}$  from the currents at a frequency of 13.56 MHz with the reference impedances being the complex conjugates of the input impedances of the antennas. Tables I and II show the input impedance and the dominant spherical mode

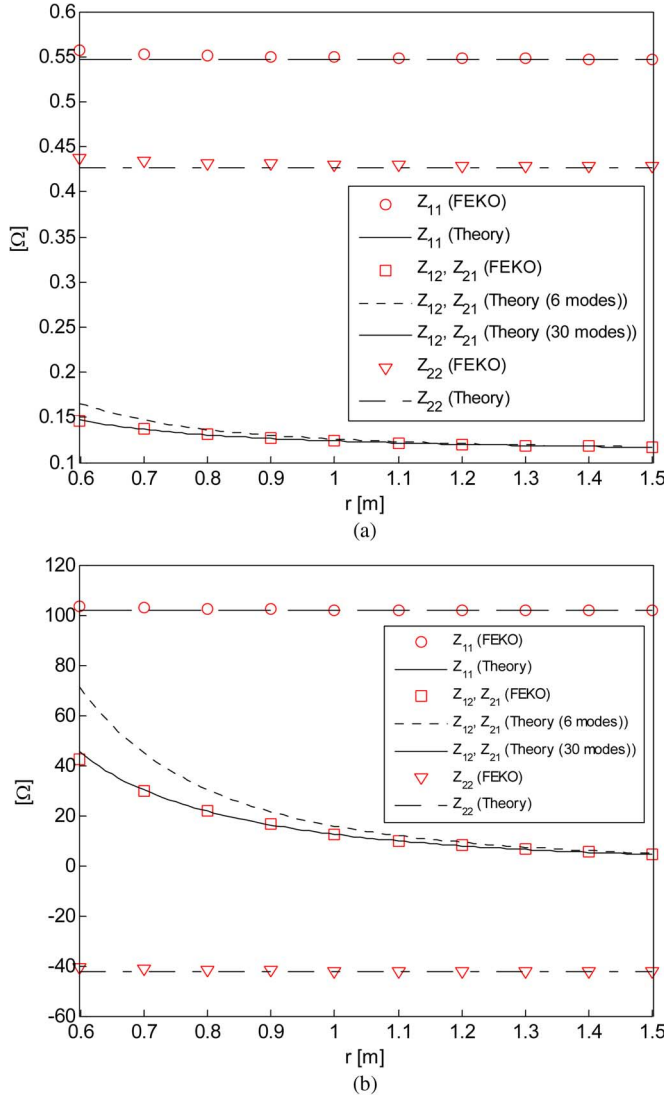


Fig. 4. Z-parameter between antenna 1 and antenna 2: (a) real part and (b) imaginary part.

coefficients among the elements of  $\mathbf{T}$  for each antenna. We assumed the four antennas to be canonical-minimum-scattering antennas and calculated  $\mathbf{S}$  using (3) and (4).

We calculated the Z-parameter between antenna 1 and antenna 2 at 13.56 MHz. In this case,  $r$  varied from 60 to 150 cm, and  $\theta$ ,  $\phi$ ,  $\phi_0$ ,  $\theta_0$ , and  $\chi_0$  were all equal to 0. The Z-parameters were calculated using (19) for six modes (maximum  $n$  of 1) and 30 modes (maximum  $n$  of 3).<sup>2</sup> We calculated the Y-parameter between antenna 3 and antenna 4 at 13.56 MHz. In this case,  $\theta$  and  $\phi$  were fixed to  $40^\circ$  and  $90^\circ$ , respectively, and  $r$  varied from 20 to 110 cm.  $\phi_0 = 90^\circ$ ,  $\theta_0 = \theta$ , and  $\chi_0 = -90^\circ$ , such that the line connecting the centers of the helices coincided with the  $z_3$ -axis, and the  $x_1$ - and  $x_3$ -axes were parallel. The Y-parameters were calculated using (20) for six modes (maximum  $n$  of 1) and 30 modes (maximum  $n$  of 3). Figs. 4 and 5 show the Z-parameter and Y-parameter values calculated using the spherical

<sup>2</sup>The number of modes written in this section indicates the number of all the modes for which the index  $n$  is not larger than the maximum value. In real calculation, the number smaller than the written number was used in all the calculations in this section.

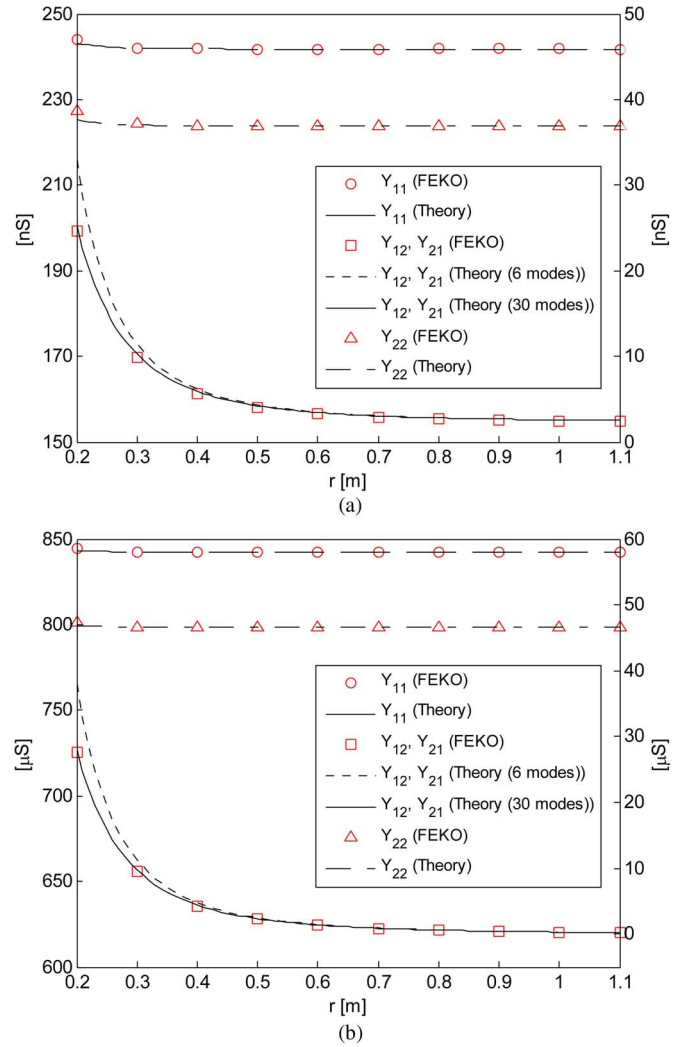


Fig. 5. Y-parameter between antenna 3 and antenna 4: (a) real part and (b) imaginary part. The left axis provides the values for  $Y_{11}$  and  $Y_{22}$ , and the right axis provides the values for  $Y_{12}$  and  $Y_{21}$ . For  $Y_{11}$  and  $Y_{22}$ , the values calculated using 6 modes and 30 modes are almost identical.

mode theory and with FEKO. The Z- and Y-parameter values obtained from the theory agree well with the values obtained using FEKO.

Using (24), we calculated the optimum load impedance from the Z-parameter obtained with FEKO for the above two cases. We terminated the feeding ports of antennas 2 and 4 with the optimum load impedance in the FEKO simulation and calculated the power transfer efficiency for the two cases. We also computed the maximum power transfer efficiency using (25) and the Z-parameter obtained with spherical modes for the two cases. Fig. 6 shows the optimum load impedance and the maximum power transfer efficiency. The maximum power transfer efficiencies calculated using the two methods agree well.

We calculated the electromagnetic field at 13.56 MHz for two configurations. For configuration 1, antenna 1 and antenna 2 were used;  $r = 1$  m, and  $\theta = \phi = \phi_0 = \theta_0 = \chi_0 = 0^\circ$ . The field was calculated using (29) for  $r_1 = 0.5$  m,  $\phi_1 = 0^\circ$ , and  $\phi_1 = 0^\circ$  to  $360^\circ$ , with the two antennas stationary.  $\phi_1 = 180^\circ$  to  $360^\circ$  and  $\phi_1 = 0^\circ$  correspond to  $\phi_1 = 180^\circ$  to  $0^\circ$  and

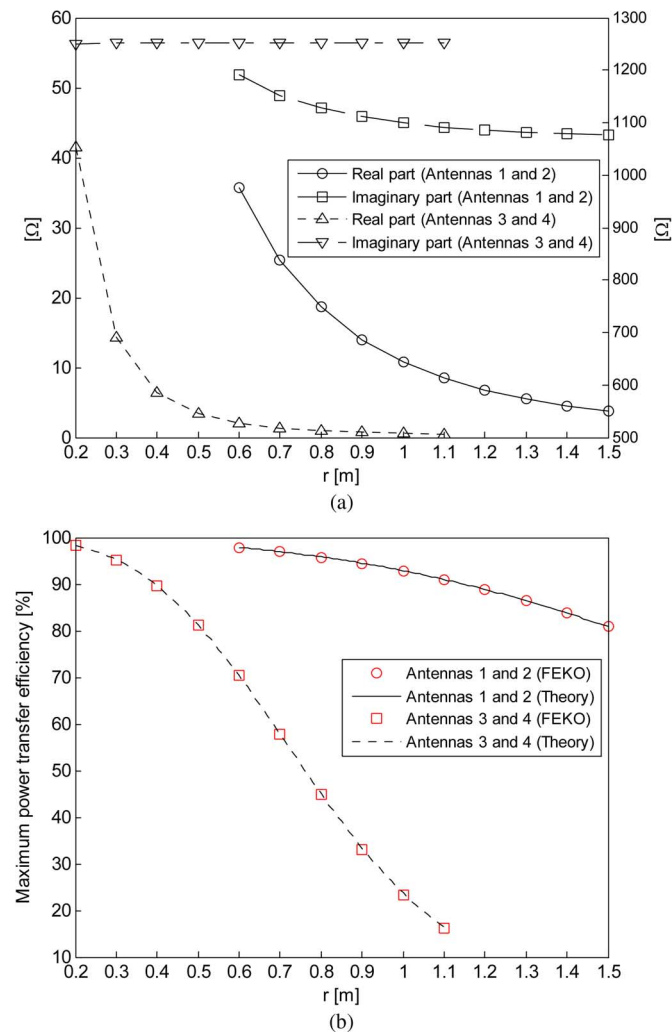


Fig. 6. (a) Optimum load impedance. The right axis provides the values for Imaginary part (Antennas 3 and 4), and the left axis provides the values for the remainder. (b) Maximum power transfer efficiency.

$\phi_1 = 180^\circ$ .  $(r_1, \theta_1, \phi_1)$  are the spherical coordinates with respect to coordinate system 1. For configuration 2, antenna 3 and antenna 4 were used;  $r = 30$  cm,  $\theta = 40^\circ$ ,  $\phi = 90^\circ$ ,  $\phi_0 = 90^\circ$ ,  $\theta_0 = 40^\circ$ , and  $\chi_0 = -90^\circ$ . The field was calculated using (28) for  $r_1 = 15$  cm,  $\phi_1 = 90^\circ$ , and  $\phi_1 = 0^\circ$  to  $360^\circ$ , with the two antennas stationary.  $\phi_1 = 180^\circ$  to  $360^\circ$  and  $\phi_1 = 90^\circ$  correspond to  $\phi_1 = 180^\circ$  to  $0^\circ$  and  $\phi_1 = 270^\circ$ . The optimum load impedance was connected to the feeding ports of antennas 2 and 4, and 10 V was applied to the feeding ports of antennas 1 and 3. When the fields were computed using the spherical mode theory, 70 modes (maximum  $n$  of 5) and 198 modes (maximum  $n$  of 9) were used for configuration 1, and 30 modes (maximum  $n$  of 3) and 126 modes (maximum  $n$  of 7) were used for configuration 2. The number of spherical modes was truncated so that the result would converge. Figs. 7 and 8 show the  $r$  components of the E-field and H-field calculated using the spherical mode theory and using FEKO. For configuration 1, the graph for the fields calculated using 198 modes and the graph for the fields calculated using FEKO coincide, and for configuration 2, the graph for the fields calculated using 126 modes and the graph for the fields calculated using FEKO coincide. The  $\theta$  component and

the  $\phi$  component of the field calculated from theory and using FEKO also agree well. We omit the presentation of graphs for the  $\theta$  component and  $\phi$  component.

## VII. CONCLUSION

Using spherical modes and an addition theorem, we derived the Z-parameter and Y-parameter between two antennas with arbitrary radiation and scattering patterns. Once we know the antenna scattering matrix of an isolated antenna, we can determine the mutual coupling between two antennas in arbitrary positions (except for the case in which the two minimum spheres that enclose the antennas overlap). We also present formulas for calculating the maximum power transfer efficiency and the optimum load impedance. We also derived a formula for calculating the electromagnetic field generated by a wireless power transfer system. We can compute the near-field and far-field values for wireless power transfer systems using this formula.

The antenna scattering matrix is calculated after the numerical computations, such as the method of moments (MOM), and this process takes time. Therefore, classical numerical methods such as MOM may be faster when the number of configurations calculated is small. When the arrangement of antennas varies and there are many configurations (the antenna structures are not changed), the method presented in this paper may be faster because in classical numerical methods, computation is performed whenever the arrangement of antennas changes, while in the proposed method, the antenna scattering matrix is calculated only once. (In the case of the example in which the Z-parameter is calculated in Section VI, the proposed method is faster when the number of configurations is greater than 2.)

Using the theory developed in this paper, we can determine the behavior of wireless power transfer solely from the parameters of an isolated antenna. For canonical-minimum-scattering antennas, we require only the modal transmitting pattern and the reflection coefficient to determine the behavior of the wireless power transfer. In addition, we can identify which parameters affect the efficiency of the wireless power transfer and find parameter values that make the wireless power transfer efficient. For example, we are able to find the radiation pattern that is efficient for wireless power transfer. Therefore, the theory proposed in this paper may be helpful in the design of efficient antennas for wireless power transfer.

## APPENDIX A

*Spherical Modes:* Electric fields and magnetic fields in a source-free region can be expressed as a linear combination of spherical modes, as follows:

$$\mathbf{E}(\mathbf{r}) = k\sqrt{\eta} \sum_{n=1}^{\infty} \sum_{m=-n}^n \left\{ a'_{mn} \mathbf{M}_{mn}^{(3)}(\mathbf{r}) + a''_{mn} \mathbf{N}_{mn}^{(3)}(\mathbf{r}) + b'_{mn} \mathbf{M}_{mn}^{(4)}(\mathbf{r}) + b''_{mn} \mathbf{N}_{mn}^{(4)}(\mathbf{r}) \right\} \quad (31a)$$

$$\mathbf{H}(\mathbf{r}) = \frac{jk}{\sqrt{\eta}} \sum_{n=1}^{\infty} \sum_{m=-n}^n \left\{ a'_{mn} \mathbf{N}_{mn}^{(3)}(\mathbf{r}) + a''_{mn} \mathbf{M}_{mn}^{(3)}(\mathbf{r}) + b'_{mn} \mathbf{N}_{mn}^{(4)}(\mathbf{r}) + b''_{mn} \mathbf{M}_{mn}^{(4)}(\mathbf{r}) \right\} \quad (31b)$$

where  $\eta$  is the intrinsic impedance,  $k$  is the wavenumber, and  $\mathbf{r}$  is the position vector. The mode functions used in this paper are

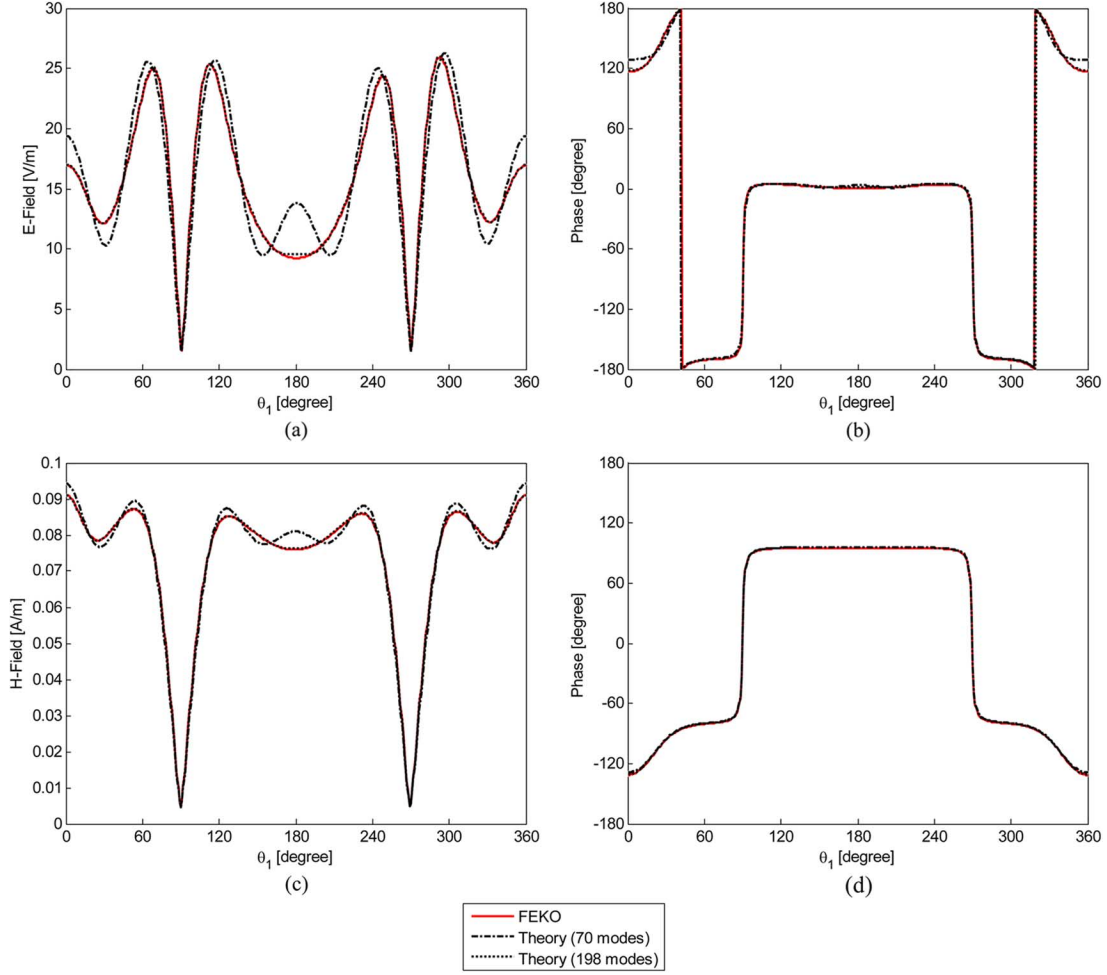


Fig. 7. Electric and magnetic fields for configuration 1. (a) Magnitude of  $r$  component of E-field. (b) Phase of  $r$  component of E-field. (c) Magnitude of  $r$  component of H-field. (d) Phase of  $r$  component of H-field.

based on the mode functions used in [7].  $\mathbf{M}_{mn}^{(c)}$  and  $\mathbf{N}_{mn}^{(c)}$  are given by the following equations:

$$\begin{aligned} \mathbf{M}_{mn}^{(c)}(\mathbf{r}) &= \left(-\frac{m}{|m|}\right)^m \sqrt{\frac{(2n+1)(n-|m|)!}{4\pi n(n+1)(n+|m|)!}} \\ &\cdot \left[ z_n^{(c)}(kr) \frac{j m P_n^{|m|}(\cos\theta)}{\sin\theta} e^{jm\phi} \hat{\theta} \right. \\ &\quad \left. - z_n^{(c)}(kr) \frac{d P_n^{|m|}(\cos\theta)}{d\theta} e^{jm\phi} \hat{\phi} \right] \end{aligned} \quad (32a)$$

$$\begin{aligned} \mathbf{N}_{mn}^{(c)}(\mathbf{r}) &= \left(-\frac{m}{|m|}\right)^m \sqrt{\frac{(2n+1)(n-|m|)!}{4\pi n(n+1)(n+|m|)!}} \\ &\cdot \left[ \frac{n(n+1)}{kr} z_n^{(c)}(kr) P_n^{|m|}(\cos\theta) e^{jm\phi} \hat{r} \right. \\ &\quad + \frac{1}{kr} \frac{d}{d(kr)} \left\{ kr z_n^{(c)}(kr) \right\} \frac{d P_n^{|m|}(\cos\theta)}{d\theta} e^{jm\phi} \hat{\theta} \\ &\quad \left. + \frac{1}{kr} \frac{d}{d(kr)} \left\{ kr z_n^{(c)}(kr) \right\} \frac{j m P_n^{|m|}(\cos\theta)}{\sin\theta} e^{jm\phi} \hat{\phi} \right] \end{aligned} \quad (32b)$$

where  $(-m/|m|)^m$  is defined as 1 when  $m = 0$ , and  $(r, \theta, \phi)$  represents spherical coordinates. Here,  $P_n^m(x)$  is the associated Legendre function; the sign of the associated Legendre function used in this paper is the same as that used in [13] and [14] but is different from that used in [7] and [15]. In  $z_n^{(c)}(kr)$ ,  $c = 1$  denotes the spherical Bessel function,  $c = 2$  denotes the spherical Neumann function,  $c = 3$  denotes the spherical Hankel function of the first kind, and  $c = 4$  denotes the spherical Hankel function of the second kind. In this study, the  $e^{j\omega t}$  time dependence is used. Therefore,  $c = 3$  indicates incoming spherical modes, and  $c = 4$  indicates outgoing spherical modes.  $a'_{mn}$  and  $b'_{mn}$  are the coefficients of the  $\text{TE}_{mn}$  modes, and  $a''_{mn}$  and  $b''_{mn}$  are the coefficients of the  $\text{TM}_{mn}$  modes. The coefficients of the outgoing spherical modes are determined using the following equation [7, p. 333]:

$$b'_{mn} = (-1)^{m+1} \int_V k \sqrt{\eta} \mathbf{M}_{-mn}^{(1)} \cdot \mathbf{J} - \frac{jk}{\sqrt{\eta}} \mathbf{N}_{-mn}^{(1)} \cdot \mathbf{M} dv \quad (33a)$$

$$b''_{mn} = (-1)^{m+1} \int_V k \sqrt{\eta} \mathbf{N}_{-mn}^{(1)} \cdot \mathbf{J} - \frac{jk}{\sqrt{\eta}} \mathbf{M}_{-mn}^{(1)} \cdot \mathbf{M} dv \quad (33b)$$

where  $\mathbf{J}$  is the electric current density,  $\mathbf{M}$  is the magnetic current density, and  $V$  is a region that contains all sources.

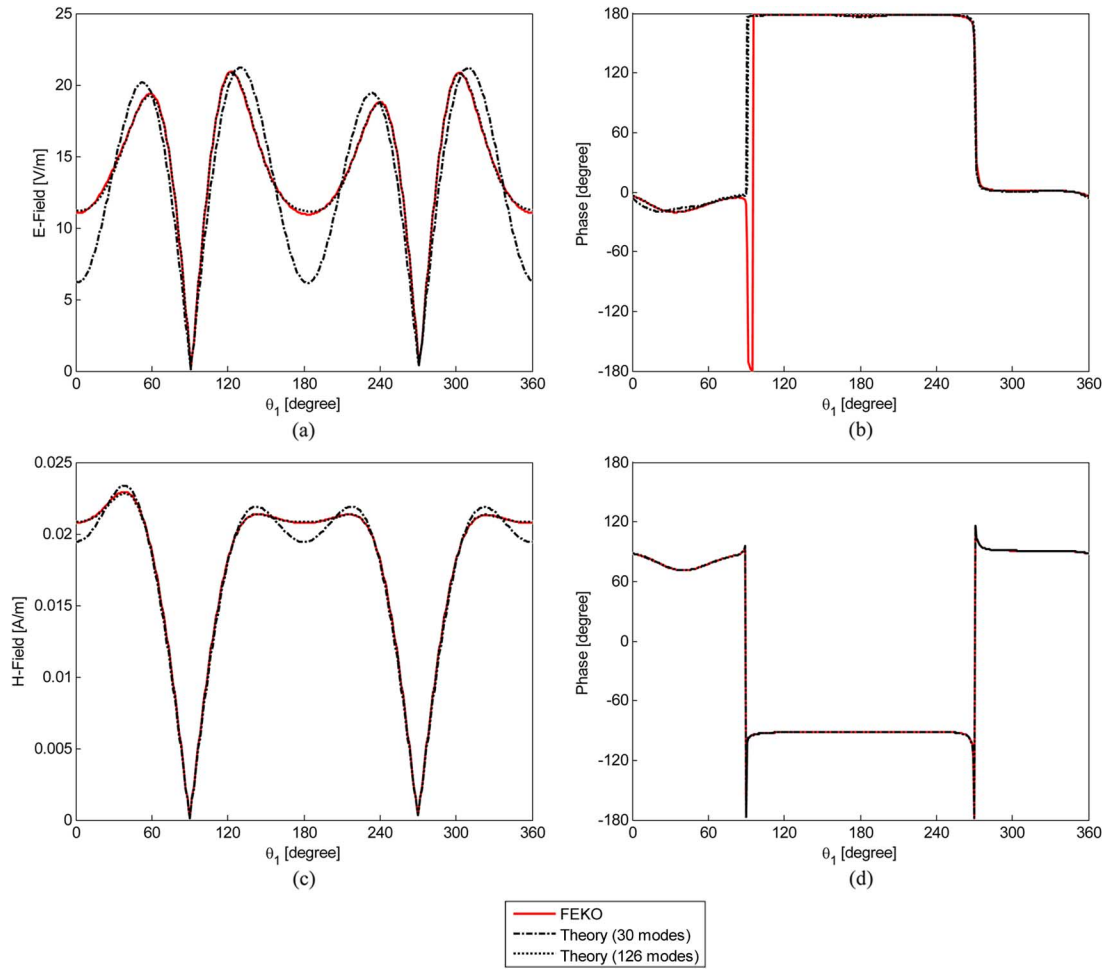


Fig. 8. Electric and magnetic fields for configuration 2. (a) Magnitude of  $r$  component of E-field. (b) Phase of  $r$  component of E-field. (c) Magnitude of  $r$  component of H-field. (d) Phase of  $r$  component of H-field.

## APPENDIX B

*Addition Theorem for Translation of Coordinates:* An addition theorem expresses mode functions in one coordinate system in terms of mode functions in another coordinate system. Coordinate system 2 is translated from coordinate system 1 by  $\mathbf{r}$ , as shown in Fig. 1.  $\mathbf{r}_1$  and  $\mathbf{r}_2$  are position vectors with respect to coordinate system 1 and coordinate system 2, respectively. The mode functions in coordinate system 1 and the mode functions in coordinate system 2 are related through the following equation:

$$\mathbf{M}_{mn}^c(\mathbf{r}_1) = \sum_{\nu=1}^{\infty} \sum_{\mu=-\nu}^{\nu} \left\{ A_{\mu\nu,mn}^{(c)}(\mathbf{r}) \mathbf{M}_{\mu\nu}^{(1)}(\mathbf{r}_2) + B_{\mu\nu,mn}^{(c)}(\mathbf{r}) \mathbf{N}_{\mu\nu}^{(1)}(\mathbf{r}_2) \right\} \quad (34a)$$

$$\mathbf{N}_{mn}^c(\mathbf{r}_1) = \sum_{\nu=1}^{\infty} \sum_{\mu=-\nu}^{\nu} \left\{ A_{\mu\nu,mn}^{(c)}(\mathbf{r}) \mathbf{N}_{\mu\nu}^{(1)}(\mathbf{r}_2) + B_{\mu\nu,mn}^{(c)}(\mathbf{r}) \mathbf{M}_{\mu\nu}^{(1)}(\mathbf{r}_2) \right\} \quad (34b)$$

for  $|\mathbf{r}_2| < |\mathbf{r}|$  and

$$\mathbf{M}_{mn}^c(\mathbf{r}_1) = \sum_{\nu=1}^{\infty} \sum_{\mu=-\nu}^{\nu} \left\{ A_{\mu\nu,mn}^{(1)}(\mathbf{r}) \mathbf{M}_{\mu\nu}^{(c)}(\mathbf{r}_2) + B_{\mu\nu,mn}^{(1)}(\mathbf{r}) \mathbf{N}_{\mu\nu}^{(c)}(\mathbf{r}_2) \right\} \quad (35a)$$

$$\mathbf{N}_{mn}^c(\mathbf{r}_1) = \sum_{\nu=1}^{\infty} \sum_{\mu=-\nu}^{\nu} \left\{ A_{\mu\nu,mn}^{(1)}(\mathbf{r}) \mathbf{N}_{\mu\nu}^{(c)}(\mathbf{r}_2) + B_{\mu\nu,mn}^{(1)}(\mathbf{r}) \mathbf{M}_{\mu\nu}^{(c)}(\mathbf{r}_2) \right\} \quad (35b)$$

for  $|\mathbf{r}_2| > |\mathbf{r}|$ , where

$$\begin{aligned} A_{\mu\nu,mn}^{(c)}(\mathbf{r}) &= (-1)^{\mu} \left( \frac{m-\mu}{|m-\mu|} \right)^{m-\mu} \frac{j^{\nu-n}}{2} \\ &\times \sqrt{\frac{(2n+1)(2\nu+1)}{n(n+1)\nu(\nu+1)}} e^{j(m-\mu)\phi} \sum_{p=|n-\nu|}^{n+\nu} \\ &\times \{ j^p (2p+1) [n(n+1) + \nu(\nu+1) - p(p+1)] \\ &\cdot \sqrt{\frac{(p-|m-\mu|)!}{(p+|m-\mu|)!}} \begin{pmatrix} n & \nu & p \\ 0 & 0 & 0 \end{pmatrix} \begin{pmatrix} n & \nu & p \\ m & -\mu & \mu-m \end{pmatrix} \\ &\cdot z_p^{(c)}(kr) P_p^{|m-\mu|}(\cos\theta) \} \end{aligned} \quad (36a)$$

$$\begin{aligned}
B_{\mu\nu,mn}^{(c)}(\mathbf{r}) &= (-1)^\mu \left( \frac{m-\mu}{|m-\mu|} \right)^{m-\mu} \frac{j^{\nu-n}}{2} \\
&\times \sqrt{\frac{(2n+1)(2\nu+1)}{n(n+1)\nu(\nu+1)}} e^{j(m-\mu)\phi} \sum_{p=|n-\nu|+1}^{n+\nu-1} \\
&\times \{ j^p (2p+1) \\
&\cdot \sqrt{(n+\nu+1+p)(n+\nu+1-p)(n-\nu+p)(\nu-n+p)} \\
&\cdot \sqrt{\frac{(p-|m-\mu|)!}{(p+|m-\mu|)!}} \begin{pmatrix} n & \nu & p-1 \\ 0 & 0 & 0 \end{pmatrix} \begin{pmatrix} n & \nu & p \\ m & -\mu & \mu-m \end{pmatrix} \\
&\cdot Z_p^{(c)}(kr) F_p^{|m-\mu|}(\cos\theta) \}. \quad (36b)
\end{aligned}$$

Here,  $((m-\mu)/(|m-\mu|))^{m-\mu}$  is defined as 1 when  $m-\mu = 0$ , and  $\begin{pmatrix} j_1 & j_2 & j_3 \\ m_1 & m_2 & m_3 \end{pmatrix}$  is the Wigner 3-j symbol [16].

### APPENDIX C

**Addition Theorem for Rotation of Coordinates:** Coordinate system 3 is rotated from coordinate system 2 (Fig. 1). The rotation of the coordinate system is expressed in terms of the Euler angles  $(\chi_0, \theta_0, \phi_0)$  [7, App. A2]. Let  $\mathbf{r}_3$  be the position vector with respect to coordinate system 3. The relation between the mode functions in coordinate system 2 and the mode functions in coordinate system 3 is expressed as follows:

$$\mathbf{M}_{mn}^{(c)}(\mathbf{r}_2) = \sum_{\mu=-n}^n D_{\mu m}^n(\chi_0, \theta_0, \phi_0) \mathbf{M}_{\mu n}^{(c)}(\mathbf{r}_3) \quad (37a)$$

$$\mathbf{N}_{mn}^{(c)}(\mathbf{r}_2) = \sum_{\mu=-n}^n D_{\mu m}^n(\chi_0, \theta_0, \phi_0) \mathbf{N}_{\mu n}^{(c)}(\mathbf{r}_3) \quad (37b)$$

where

$$D_{\mu m}^n(\chi_0, \theta_0, \phi_0) = (-1)^{m-\mu} e^{jm\phi_0} d_{\mu m}^n(\theta_0) e^{j\mu\chi_0} \quad (38)$$

with  $d_{\mu m}^n(\theta_0)$  defined as in [7, p. 345].

### REFERENCES

- [1] W. C. Brown, "The history of power transmission by radio waves," *IEEE Trans. Microw. Theory Techn.*, vol. 32, no. 9, pp. 1230–1242, Sep. 1984.
- [2] A. Karalis, J. D. Joannopoulos, and M. Soljacic, "Efficient wireless non-radiative mid-range energy transfer," *Ann. Phys.*, vol. 323, no. 1, pp. 34–48, Jan. 2008.
- [3] P. Sample, T. Meyer, and R. Smith, "Analysis, experimental result, and range adaptation of magnetically coupled resonators for wireless power transfer," *IEEE Trans. Ind. Electron.*, vol. 58, no. 2, pp. 544–554, Feb. 2011.

- [4] T. Imura and Y. Hori, "Maximizing air gap and efficiency of magnetic resonant coupling for wireless power transfer using equivalent circuit and Neumann formula," *IEEE Trans. Ind. Electron.*, vol. 58, no. 10, pp. 4746–4752, Oct. 2011.
- [5] I. Awai and T. Komori, "A simple and versatile design method of resonator-coupled wireless power transfer system," in *Proc. 2010 Int. Conf. Commun., Circuits, Syst.*, pp. 616–620.
- [6] J. Lee and S. Nam, "Fundamental aspects of near-field coupling small antennas for wireless power transfer," *IEEE Trans. Antennas Propag.*, vol. 58, no. 11, pp. 3442–3449, Nov. 2010.
- [7] J. E. Hansen, *Spherical Near-field Antenna Measurements*. Stevenage, U.K.: Peregrinus, 1988.
- [8] J. Rubio, M. A. Gaonzalez, and J. Zapata, "Generalized-scattering-matrix analysis of a class of finite arrays of coupled antennas by using 3-D FEM and spherical mode expansion," *IEEE Trans. Antennas Propag.*, vol. 53, no. 3, pp. 1133–1144, Mar. 2005.
- [9] W. Wasylkiwskyj and W. K. Kahn, "Scattering properties and mutual coupling of antennas with prescribed radiation pattern," *IEEE Trans. Antennas Propag.*, vol. 18, no. 6, pp. 741–752, Nov. 1970.
- [10] D. M. Pozar, *Microwave Engineering*, 4th ed. New York, NY, USA: Wiley, 2012, p. 186.
- [11] W. K. Kahn and H. Kurss, "Minimum-scattering antennas," *IEEE Trans. Antennas Propag.*, vol. 13, no. 5, pp. 671–675, Sep. 1965.
- [12] J. Rubio and J. F. Izquierdo, "Relation between the array pattern approach in terms of coupling coefficients and minimum scattering antennas," *IEEE Trans. Antennas Propag.*, vol. 59, no. 7, pp. 2532–2537, Jul. 2011.
- [13] R. F. Harrington, *Time-Harmonic Electromagnetic Fields*. New York, NY, USA: McGraw-Hill, 1961, Appendix E.
- [14] M. Abramowitz and I. A. Stegun, *Handbook of Mathematical Functions*. New York, NY, USA: Dover, 1965, ch. 8.
- [15] J. A. Stratton, *Electromagnetic Theory*. New York, NY, USA: McGraw-Hill, 1941, ch. 7.
- [16] A. R. Edmonds, *Angular Momentum in Quantum Mechanics*, 2nd ed. Princeton, NJ, USA: Princeton Univ. Press, 1974, ch. 3.



**Yoon Goo Kim** received the B.S. and M.S. degrees in electronic engineering from Seoul National University, Seoul, Korea, in 2009 and 2011, respectively. He is currently working toward the Ph.D. degree at Seoul National University.

His main research interests include theoretical analysis wireless power transfer system and characteristic mode.



**Sangwook Nam** (S'87–M'88–SM'11) received the B.S. degree from Seoul National University, Seoul, Korea, in 1981, the M.S. degree from the Korea Advanced Institute of Science and Technology (KAIST), Seoul, Korea, in 1983, and the Ph.D. degree from The University of Texas at Austin, Austin, TX, USA, in 1989, all in electrical engineering.

From 1983 to 1986, he was a Researcher with the Gold Star Central Research Laboratory, Seoul, Korea. Since 1990, he has been a Professor with the School of Electrical Engineering and Computer Science, Seoul National University. His research interests include analysis/design of electromagnetic (EM) structures, antennas, and microwave active/passive circuits.